Astron. Astrophys. 279, 179–187 (1993)

ASTRONOMY AND ASTROPHYSICS

The discovery and properties of the ultra-soft X-ray transient EXO 1846-031

A.N. Parmar[1], **L. Angelini**[2,3], **P. Roche**[4], **and N.E. White**[2]

[1] Astrophysics Division, Space Science Department of ESA, NL-2200 AG Noordwijk, The Netherlands
[2] Laboratory for High Energy Astrophysics, NASA Goddard Space Flight Center, Greenbelt, MD 20771, USA
[3] Universities Space Research Association
[4] Department of Physics, University of Southampton, Southampton, SO9 5NH, UK

Received May 8, accepted June 20, 1993

Abstract. We report the discovery of a previously uncatalogued *ultra-soft* X-ray transient EXO 1846-031 which was in outburst during 1985 April to September. The X-ray spectrum consists of an *ultra-soft* component and a high-energy power-law tail that extends to at least 25 keV. The *ultra-soft* component may be modeled by either a cutoff power-law or a multicolor blackbody disk model. The latter model allows the evolution in spectrum and intensity observed during the outburst to be accounted for by the change in a single parameter - the temperature at the innermost disk radius. We demonstrate that at least one other accretion disk model is able to account for these changes by the variation of a single parameter. During one of the three EXOSAT observations, EXO 1846-031 exhibited significant intensity variability which probably originates from the power-law component. We derive a position for this unidentified source and present the results of a search for the optical counterpart.

Key words: stars: individual: EXO 1846-031 – X-rays: bursts – X-rays: stars – accretion disks – black hole physics

1. Introduction

The study of X-ray transients in outburst provides a unique insight into the dependence on luminosity of the accretion process in X-ray binary systems (e.g. Gottwald et al. 1986; Parmar et al. 1989a,b). These systems are also unique in that once an outburst has ended, they allow the properties of a system to be investigated without the effects of the X-ray emission being present (e.g. McClintock & Remillard 1986; Callanan & Charles 1991). The spectral properties of transient X-ray sources have been considered by White et al. (1984), building on earlier work by Cominsky et al. (1978) and Maraschi et al. (1976). Three classes of spectral behavior are observed that can be classified by their 2–10 keV spectral shape as *hard*, *soft*, or *ultra-soft*. The *hard* transients are generally X-ray pulsars and are often associated with early-type stellar companions. Many of the *soft* transients undergo X-ray bursts and are identified with faint blue optical counterparts indicating that they are related to the low-mass X-ray binaries. The *ultra-soft* transients show extremely soft X-ray spectra below 10 keV while at high energies they may have power-law tails that extend out to at least 100 keV (e.g. H 1705-25; Wilson & Rothschild 1983, GS 1124-68; Sunyaev et al. 1992). The only spectral analogy for these objects amongst the persistent sources is that of the accreting black hole candidates such as Cyg X-1, LMC X-1 and LMC X-3.

It is still not clear which (if any) X-ray characteristics are unique to black holes. A number of properties once believed to be typical of accreting stellar black holes such as very soft spectra, fast variability and high energy tails are now known to occur in neutron star systems as well (e.g. Tanaka 1992). The strongest evidence that *ultra-soft* transients, as a class, contain black holes comes from radial velocity measurements. These allow the mass functions and hence lower limit masses of the compact objects to be determined. The *ultra-soft* transient that is probably the best studied in the optical is A 0620-00. In this system the lower limit to the mass of the compact object is $2.9M_{\odot}$ (McClintock & Remillard 1986). Recently, mass functions of $6.3 \pm 0.3M_{\odot}$ and $3.1 \pm 0.4M_{\odot}$ have been determined for GS 2023+33 and GS 1124-68, respectively (Casares et al. 1992; Remillard et al. 1991). Since these exceed the maximum mass of a stable neutron star, it is likely that these systems contain black holes. In contrast, no evidence exists that any of the compact objects associated with the *hard* or *soft* transients or their persistent counterparts exceeds $2M_{\odot}$ (Bahcall 1978; Nagase 1989). Thus, it is likely that *ultra-soft* transients as a class contain black holes.

It is therefore important to study the X-ray properties of the small number of objects in this class in order to determine if there are characteristics that are unique to black holes and to further understand the physics of accretion onto these objects. In

Send offprint requests to: A.N. Parmar

this *paper* we report on the discovery of a previously unknown *ultra-soft* transient EXO 1846-031. We discuss its temporal and spectral properties and provide a precise position for the source. We compare the properties of EXO 1846-031 with those of other *ultra-soft* transients.

2. Observations

When the EXOSAT optical axis was moved between scheduled pointing directions, the medium energy detector array (ME; Turner et al. 1981) and gas scintillation proportional counter (Peacock et al. 1981) were operated primarily to provide a monitor of the background counting rate. The 45′ full width half-maximum field of view (FOV) of the detectors occasionally passed over an X-ray source which was detected using methods similar to those employed in previous all-sky survey programs (e.g. Warwick et al. 1981; Wood et al. 1984). The normal slew maneuvering rate of 44° h^{-1} gave an exposure time of $\sim$ 1 minute for a point source and allowed a bright source to be positioned to a precision of $\sim$ 3′ along the direction of motion and $\pm$45′ perpendicular to it. Many of these detections corresponded to previously catalogued sources, but several were new transient sources (White & Peacock 1985 and references therein).

On 1985 April 2 at 17:54 UT a bright ($\sim$ 400 ME counts s^{-1}), uncatalogued X-ray source was detected during a slew. A follow-up pointed observation starting on 1985 April 3, showed that the spectrum was characteristic of an *ultra-soft* transient. A channel multiplier array (CMA) detector at the focus of one of the two imaging telescopes on EXOSAT (de Korte et al. 1981) was used to obtain a preliminary position of RA: $18^h\ 46^m\ 39^s$, decl. −03°07′34″ (epoch 1950) with an uncertainty radius of 15″. The new source was designated EXO 1846-031 (Parmar & White 1985).

A total of three pointed EXOSAT observations of EXO 1846-031 were made between 1985 April 3 and September 7 (Table 1). The count rate in the ME detector decreased from observation to observation with a $1/e$ time scale of $\sim$ 85 days suggesting that the decline of an outburst was being observed. During each observation four of the eight ME detectors were offset by 2° to provide a simultaneous monitor of the background count rate. Approximately half way through each observation, the pointing positions of the two detector halves were interchanged and all ME count rates in this *paper* refer to four argon detectors observing the source.

Table 1. Log of observations

Observation number	Start (1985) day h:m	Duration h:m	ME Count rate[a] (1–10 keV)
1	Apr 3 21:53	4:58	602.8 ± 1.5
2	May 2 02:00	2:30	447.4 ± 1.2
3	Sep 7 18:46	6:07	86.7 ± 0.3

[a]Corrected for collimator transmission assuming the mean CMA source position obtained from observations 1 and 3.

2.1. Source position

In the case of the EXO 1846-031 observations reported here, the determination of the best estimate source position is complicated by a number of factors: (1) during the first observation the EXOSAT pointing direction was changed in order to bring the source closer to the center of the field of view (FOV) at 1985 April 4 00:12 UT. This allows the source position to be determined twice, although one determination has a significantly larger uncertainty due to the less well determined point response profile at an off-axis angle of 17′. (2) during part of the second observation the spacecraft lost stable pointing for $\sim$ 20 minutes and drifted off-target. (3) There appears to have been a misidentification of the single guide star used to determine the position of the EXOSAT boresight. This resulted in the position derived from the second observation being $\sim$ 20′ from those determined from the first and third observations (Table 2). We note that the 7″ uncertainty radius given in Gottwald et al. (1991) for EXO 1846-031 underestimates the systematic uncertainties in CMA source position determination. During a second slew maneuver on 1985 April 29 at 04:17 UT the spacecraft pointing axis passed over EXO 1846-031 moving in a direction approximately perpendicular to that during the discovery slew. The combined uncertainty region is $\sim$ 3′ square and clearly excludes the source positions derived from the second pointed observation. This confirms that the guide star was misidentified during the second observation. Taking the average of the positions obtained from the first and third observations gives a best position for EXO 1846-031 of RA: $18^h\ 46^m\ 39.6^s$, decl. −03°07′21″ (epoch 1950) with a 90% confidence uncertainty radius of 11″.

Figure 1 shows an I-band CCD finding chart of the region of sky covering the uncertainty regions derived from the first and third observations. The chart was obtained using the 1 meter Jacobus Kapteyn telescope (JKT) on La Palma on 1992 July 27, with an EEV 1280 x 1180 pixel CCD. In addition, V and R band exposures of the same field were made. The data were reduced using the Starlink KAPPA, FIGARO and PHOTOM packages and calibrated using observations of Landolt (1992) standards. The limiting magnitudes are $\sim$ 22 for each of the exposures. The three EXOSAT uncertainty regions are indicated. We have examined the color ratios of stars 1 to 58 and do not find any with unusual values.

For completeness, we also examined the region of sky containing the uncertainty regions determined from the second observation. V, R, and I-band exposures were made on 1992 November 2 using the same equipment as before. Lower exposure times result in limiting magnitudes of $\sim$ 20. The color ratios of the brightest 12 stars within and around the CMA uncertainty regions do not show any anomalous values.

2.2. X-ray lightcurves

The 1–10 keV background subtracted light curves for each observation are plotted in Fig. 2 with a time resolution of 40 s. The plots are scaled such that the ordinate extrema represent ±25%

Table 2. EXO 1846-031 Position Determinations

Obs	Start Time (1985) day h:m	Exposure h:m	CMA Filter[a]	Off axis Angle ′	CMA Count Rate s^{-1}	RA (1950) h m s	Dec d ′ ″	90% Conf. Uncertainty Radius (″)
1	Apr 3 22:40	1:21	3000ÅLex	17	0.100 ± 0.009	18 46 39.6	−03 07 23	27
1	Apr 4 00:36	0:03	3000ÅLex	1	0.134 ± 0.032	18 46 39.3	−03 07 28	15
2	May 2 02:47	0:36	3000ÅLex	19	0.065 ± 0.008	18 45 26.7	−03 25 38	19
2	May 2 03:40	0:22	Al/Pa	19	0.039 ± 0.008	18 45 26.9	−03 25 41	18
3	Sep 7 19:36	4:46	3000ÅLex	4	0.027 ± 0.002	18 46 39.8	−03 07 12	15

[a] See de Korte et al. (1981) for a description of the CMA filters.

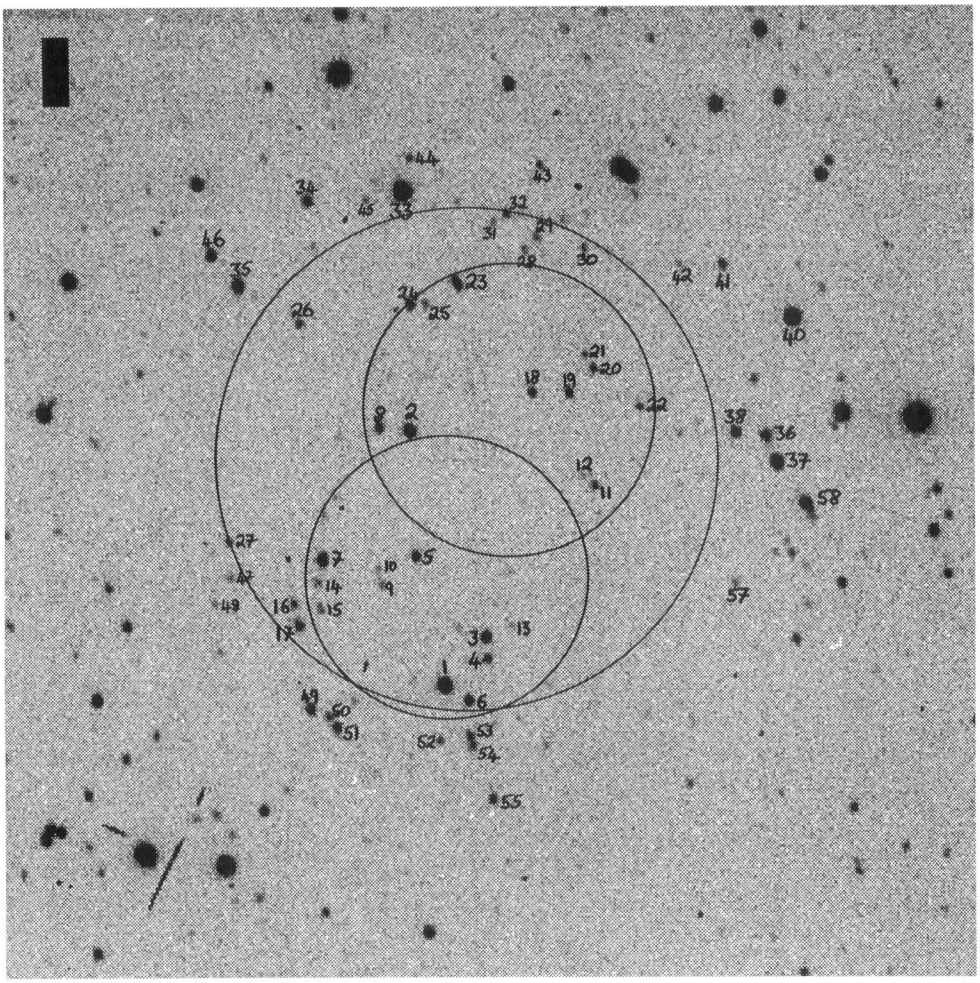

Fig. 1. An I-band finding charts for EXO 1846-031. North is at the top and East to the left. The field covers an area $\sim$ 3′ x 3′ and has a limiting magnitude of $\sim$ 22. The exposure time is 600 s

variations in source intensity for each observation. The average ME 1–10 keV count rates for each observation are given in Table 1. These have been corrected for the 45′ FWHM collimator efficiency of the ME using the mean source position obtained from the first and third observations. This results in a correction factor of 1.45 for the second observation. During the first two observations the light curves do not show any obvious variability, whereas in the third observation there is evidence for marked intensity variations. To quantify this variability we estimated the *rms* excess variability ϵ, corrected for sampling effects and counting statistics, defined as $((\sigma^2_{obs} - \sigma^2_{exp})^{0.5}/X)$, where σ^2_{obs} is the observed variance, σ^2_{exp} is the expected variance from a constant source, and X the mean count rate. In the 1–10 keV energy band ϵ is $0.5 \pm 0.1\%$, $0.5 \pm 0.2\%$ and $4.0 \pm 0.2\%$ in the first, second, and third observations, respectively. The background data taken simultaneously show that the contribution to the variability from the background in the same energy range is $< 0.1\%$ for the first two observation and $< 0.4\%$ for the third observation. In order to confirm that we do not observe excess variability from a constant source, we analyzed 2 h of 1–10 keV ME data from the Crab Nebula and set a limit to any excess variability of $< 1\%$ for a time scale of > 40 s. This confirms that the

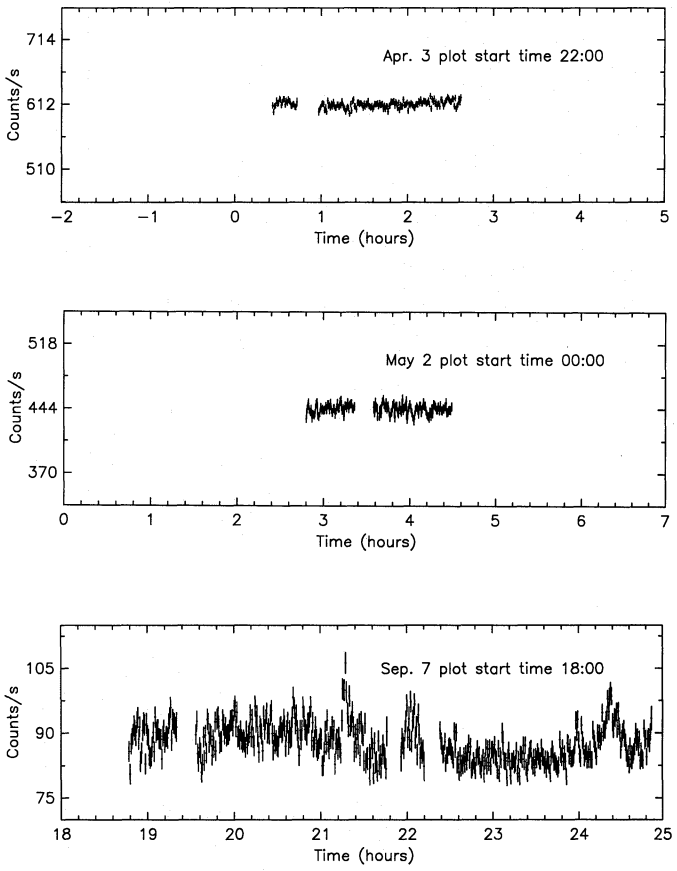

Fig. 2. EXOSAT ME 1–10 keV lightcurves of the three observations of EXO 1846-031 plotted with a time resolution of 40 s. In each plot the ordinate extrema represent variability of ±25% from the mean. Flaring activity during the 1985 September 7 observation is visible

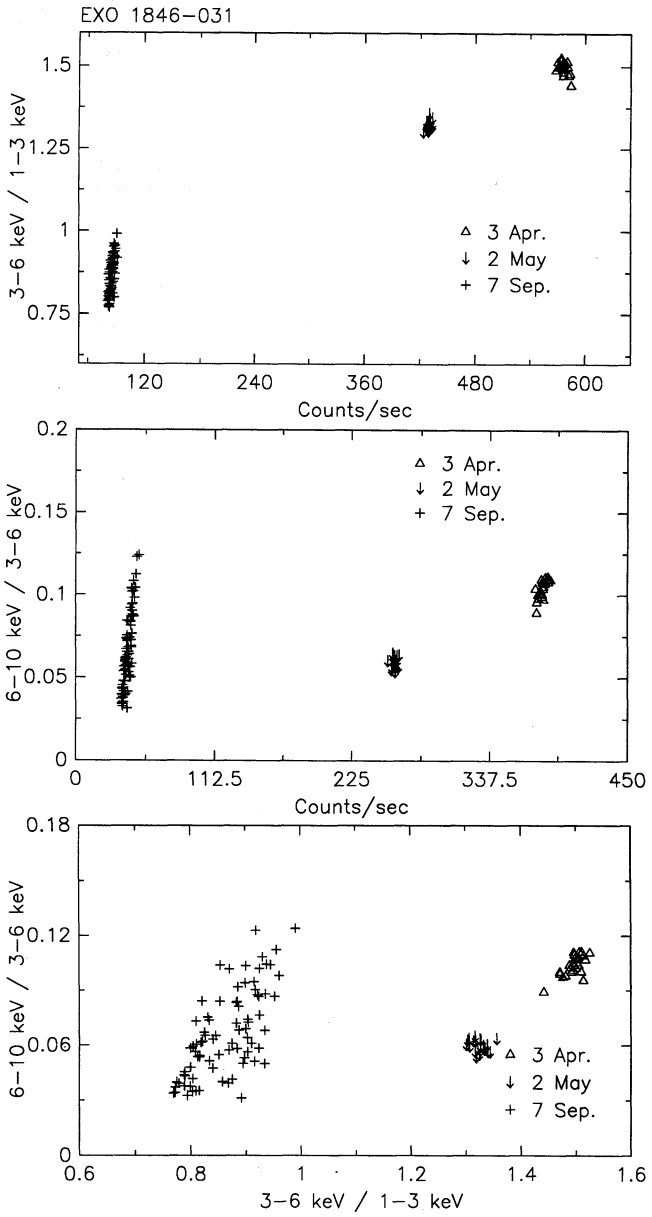

Fig. 3. The upper panel shows the the *softness* ratio (counts in the 3–6 keV band divided by those in the 1–3 keV band) versus 1–6 keV intensity while the middle panel shows the *hardness* ratio (counts in the 6–10 keV band divided by those in the 3–6 keV band) versus 3–10 keV intensity. The lower panel is a color-color diagram (i.e. the *hardness* ratio plotted against the *softness* ratio). In all three cases, each point represents an integration over an interval of 250 s

excess variability detected in the 1985 September 7 observation originates from EXO 1846-031.

The energy dependence of this variability was investigated by accumulating light curves for each observation in the energy bands 1–3, 3–6, and 6–10 keV. Two count ratios were obtained; a *softness* ratio (counts in the 3–6 keV band divided by those in the 1–3 keV band) and a *hardness* ratio (counts in the 6–10 keV band divided by those in the 3–6 keV band). The upper and middle panels of Fig. 3 show each ratio versus the total intensities in each energy band. The lower panel shows a color-color diagram (i.e. the *hardness* ratio versus the *softness* ratio). Each point represents an integration over an interval of 250 s. Both the *softness* and *hardness* ratios decrease as the source intensity decays during the outburst. However, during the third observation there is considerable variability in both ratios. The magnitude of this variability is comparable with that seen during the decay and is larger for the *hardness* ratio than the *softness* ratio. The amplitude of the hard band variations observed during the third observation is comparable to the change in the *hardness* ratio that occurred between the other two observations.

To further investigate the variability seen in the third observation we computed auto correlation functions (ACFs) by averaging the ACFs obtained from intervals of 1920 s with a resolution of 30 s in four energy bands. The ACFs in the energy range 1–10 keV for the first two observations are consistent with zero correlations at any (non-zero) time lag in the range investigated. The 1–10 keV ACF of the third observation shows an exponential decay with a characteristic time scale of $\sim$ 50 s (Fig. 4). The ACFs for the energy ranges 1–3, 3–6, and 6–10 keV for the third observation are also shown in Fig. 4. The 1–3 keV energy range ACF does not show any correlation for

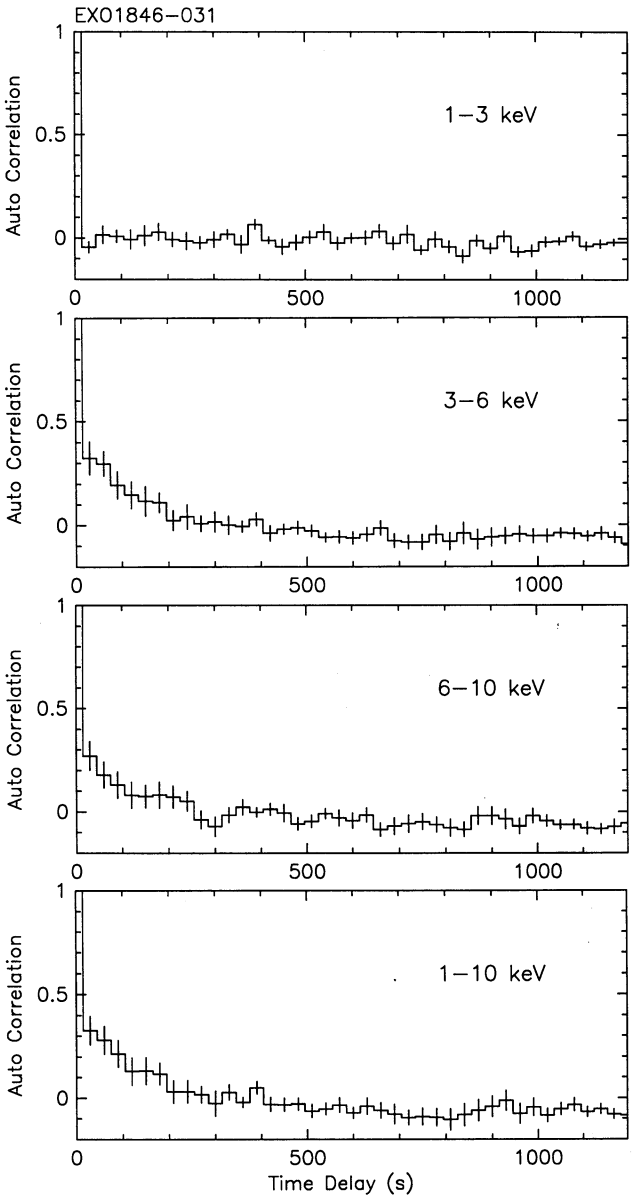

Fig. 4. Auto correlation functions (ACFs) for the 1985 September 7 observation obtained by averaging the ACFs obtained from 1920 s intervals of data with a resolution of 30 s

any non-zero time lags. The other ACFs are consistent with exponential shapes with e-folding time delays of $84\pm^{25}_{20}$ s and $30\pm^{10}_{7}$ s for the energy ranges 3–6 and 6–10 keV, respectively. This exponential shape is expected in a shot noise model consisting of Poisson distributed exponential decay (or rise) shots, with a sharp rise (or decay) (Sutherland et al. 1978). In such models the e-folding time delay of the ACF corresponds to the decay time of the shots.

2.3. X-ray spectrum

For the first two observations 64 channel pulse height analyzer spectra were obtained from the argon chamber of the ME every 1 s. During the third observation 128 channel pulse height analyzer argon spectra were obtained every 10 s. These data were summed and the background subtracted to provide an average spectrum for each observation. These were then fit using single component power-law, thermal bremsstrahlung, blackbody, cutoff power-law with photon index Γ (i.e. $E^{-\Gamma}\exp^{-E/kT}$), unsaturated Comptonized disk (Sunyaev & Titarchuk 1980) and multicolor blackbody disk (Mitsuda et al. 1984) models. Low-energy absorption using the coefficients of Morisson & McCammon (1983) was added to the above models. The Mitsuda et al. (1984) disk model was chosen to allow comparison with recent *Ginga* results where changing a single parameter in this model successfully accounts for the spectral and luminosity variations observed during the outbursts of two *ultra-soft* transients GS 2000+25 and GS 1124-68 (Tanaka et al. 1992; Kitamoto et al. 1992). All the trial models gave unacceptable fits to all three spectra. Of the above models, the cutoff power-law came closest to being acceptable with χ^2's per degree of freedom (dof) of 366/61, 106/61 and 276/122 for observations 1, 2 and 3, respectively. Examination of the differences between the observed counts and those predicted by each of the above models suggests that line emission is not responsible for the poor fits and that a more complex continuum model is required. If a power-law component of photon index, $\alpha_{\rm PL}$, is added to the above best-fit model, then acceptable fits to all three spectra are obtained (Table 3). The model photon distribution, $f(E)$, is then of the form:

$$f(E) = (\mathrm{a}_1 E^{-\Gamma}\exp^{-E/kT} + \mathrm{a}_2 E^{-\alpha_{\rm PL}})$$
$$\exp^{-N_{\rm H}\sigma_{\rm MM}} \qquad \text{photons cm}^{-2}\ \text{s}^{-1} \qquad (1)$$

where $\sigma_{\rm MM}$ are the photoelectric absorption coefficients of Morisson & McCammon (1983), $N_{\rm H}$ the equivalent hydrogen column density and a_1 and a_2 are the normalizations of the cutoff power-law (soft) and the power-law (hard) components, respectively. During the first observation, the 90% confidence upper limit to a 1 keV FWHM emission feature at 6.5 keV is 140 eV. We note that the functional form of the hard component is not well defined by the EXOSAT data and acceptable fits can also be obtained if e.g. a thermal bremsstrahlung component is substituted for the power-law in Equation (1). We nevertheless show the results of the fits using the above model in Table 3 to allow comparison with other sources. Note that all uncertainties in this *paper* are quoted at 90% confidence (χ^2_{min} + 2.7 for one parameter of interest). Table 3 indicates that the overall luminosity of EXO 1846-031 decreased by a factor $\sim$ 7 over an interval of 150 days. For an exponential decay this corresponds to a reduction in intensity by a factor of e every $\sim$ 85 days. The luminosity of the hard (power-law) component decreased more rapidly than that of the soft component between the first and second observations and then changed more slowly. Note that in all cases a power-law component is required in order to obtain satisfactory fits.

The multicolor blackbody disk model of Mitsuda et al. (1984) plus a power-law hard component have been satisfactorily fit to the observed spectra of the black hole candidates LMC

Table 3. Cutoff power-law spectral fit results

Observation	1	2	3	Units
Date (1985)	Apr 3-4	May 2	Sep 7	
a_1	8.6 ± 2.5	$5.79\pm^{1.01}_{0.02}$	$3.10\pm^{1.70}_{1.15}$	photons cm^{-2} s^{-1}
Γ	0.03 ± 0.50	-0.74 ± 0.28	$-0.94\pm^{0.12}_{1.04}$	
kT	1.15 ± 0.15	0.92 ± 0.06	0.67 ± 0.15	keV
a_2	$1.43\pm^{3.00}_{0.01}$	$0.0007\pm^{0.0105}_{0.0006}$	$0.052\pm^{0.254}_{0.040}$	photons cm^{-2} s^{-1}
α_{PL}	2.35 ± 0.45	0.09 ± 1.02	1.865 ± 0.80	
N_H	3.65 ± 0.20	3.10 ± 0.20	2.76 ± 0.52	$\times 10^{22}$ atoms cm^{-2}
χ^2/dof	70.8/58	66.0/58	136.2/119	
Luminosity[a]	10.0	5.86	1.45	$\times 10^{37}$ ergs s^{-1}
L_{Soft}/L^b_{Hard}	1.4–4.0	31–41	3.6–11.5	

[a] In the energy range 1–25 keV for a distance of 7 kpc (see text) and assuming that the observed absorption is interstellar. The spectral model and the meaning of the parameters are described in Equation (1).
[b] In the energy range 1–25 keV.

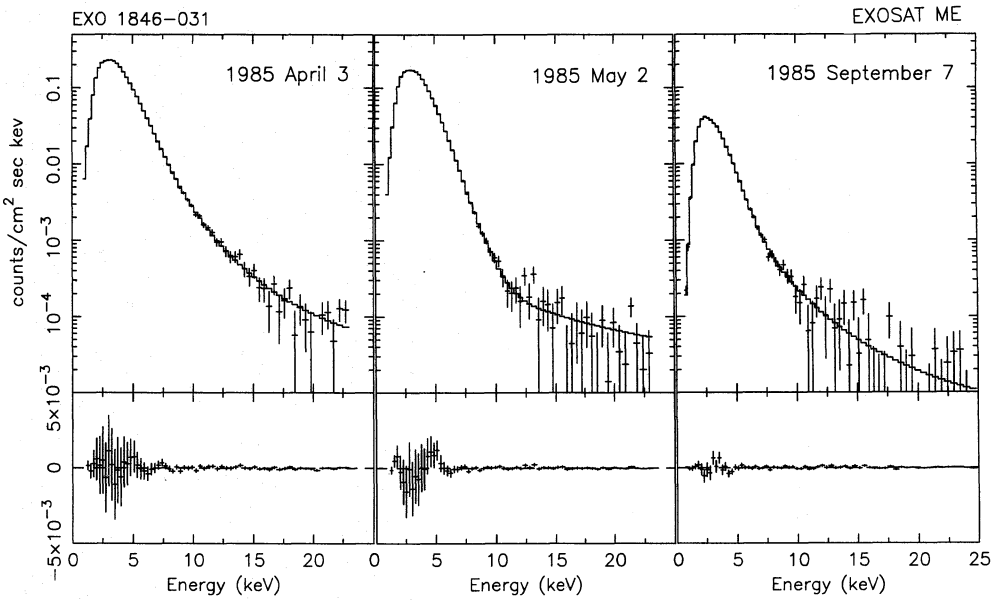

Fig. 5. The upper panels show observed and best-fit multicolor blackbody disk and power-law model count spectra for each of the EXOSAT observations. The best-fit parameters are given in Table 4. The lower panels show the residuals from the best fits

X-1, LMC X-3 (Ebisawa et al. 1991), GX 339-4 (Miyamoto et al. 1991), GS 2000+25 (Tanaka 1992) and GS 1124-68 (Kitamoto et al. 1992). This model assumes that the gravitational energy released by the accreting material is locally dissipated into blackbody radiation, that the accretion flow is continuous throughout the disk and that the effects of electron scattering on the spectrum are negligible. (The latter assumption is only valid for accretion rates < 0.001 of Eddington (White et al. 1988)). The energy spectrum is given by the surface integral of the blackbody spectra. There are only two parameters in the model; $R_{in}(\cos\theta)^{0.5}/d_7$ where R_{in} is the innermost radius of the disk in km, θ the inclination angle of the disk, d_7 the source distance in units of 7 kpc, and T_{in} the blackbody effective temperature at R_{in}. As before, we include a power-law with a photon index α_{PL} and normalization a_2 in the fits. The results of fits to the same spectra as above are presented in Table 4. The reduced χ^2 values are comparable to those obtained using the cutoff power-law model. This means that goodness of fit cannot be used to discriminate between the two spectral models. Figure 5 shows the observed and model count spectra and the residuals for each observation. The good quality of the fits and the overall change in the spectrum from observation to observation are evident. A clear trend in T_{in} is evident with a decrease from 0.96 keV to 0.69 keV during an interval when the luminosity decreased by a factor ~ 7. In contrast, the values of $R_{in}(\cos\theta)^{0.5}/d_7$ appear uncorrelated with luminosity and change from ~ 22 km by less than 0.7 km over the same interval. Both the cutoff power-law and multicolor blackbody disk model fits show evidence for a decrease in N_H of $\sim 10^{22}$ atoms cm^{-2} as the outburst evolved. We caution that this may be due to inadequacies in the spectral models. Figure 6 shows the photon spectrum derived assuming the best-fit parameters given in Table 4 for the first observation. The contributions from the multicolor blackbody disk and power-law components are indicated separately. It can be seen that the power-law dominates the spectrum at energies $\gtrsim 7$ keV.

Table 4. Multicolor blackbody disk spectral fit results

Observation	1	2	3	Units
Date (1985)	Apr 3-4	May 2	Sep 7	
$R_{in}(\cos\theta)^{0.5}/d_7$	21.62 ± 0.70	23.18 ± 0.55	21.6 ± 1.5	km
T_{in}	0.964 ± 0.017	0.929 ± 0.006	0.695 ± 0.017	keV
a_2	$2.98 \pm^{2.57}_{1.34}$	$0.00031 \pm^{0.00228}_{0.00025}$	$0.0355 \pm^{0.076}_{0.002}$	photons cm^{-2} s^{-1}
α_{PL}	2.64 ± 0.26	-0.22 ± 0.88	1.79 ± 0.55	
N_H	3.76 ± 0.21	3.57 ± 0.06	3.14 ± 0.13	$\times 10^{22}$ atoms cm^{-2}
χ^2/dof	69.4/59	69.9/59	135.3/120	

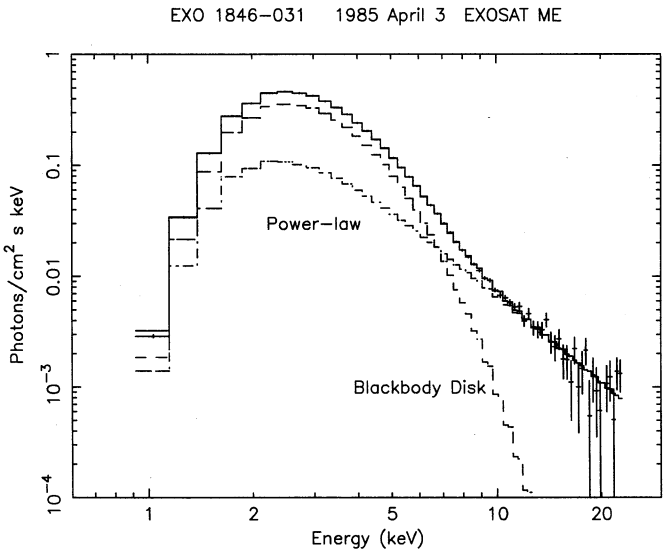

Fig. 6. The derived photon spectrum observed from EXO 1846-031 during the first observation. The spectrum has been obtained using the multicolor blackbody disk and power-law model with the best-fit parameters given in Table 4

In order to investigate whether other accretion disk spectral models are able to similarly model the observed spectral changes, we fit the Shakura & Sunyaev (1973) and Stella & Rosner (1984) modified blackbody disk models in conjunction with power-law components to the EXO 1846-031 spectra. We use the same values of the disk α and compact object mass as White et al. (1988). The fits of both these models are of poorer quality than the cutoff power-law and multicolor blackbody disk fits, with typical reduced χ^2's of ~ 2. However, the fits using the Stella & Rosner (1984) model show a similar dependency as the multicolor blackbody disk fits, with the change in spectrum and luminosity being accounted for by a decrease in mass accretion rate. The second parameter in the fits $(d/(\cos\theta)^{0.5})$ remains essentially constant during the outburst. The fits of the Shakura & Sunyaev (1973) model do not give a clear separation of dependency. We therefore conclude that the ability of the Mitsuda et al. (1984) model to successfully account for the changes in source properties during the outburst using only one parameter is not unique.

2.4. Spectral variability during flares

The spectral properties of the flaring observed during the third observation were investigated by accumulating two background subtracted spectra covering non-flaring (1985 September 7 22:21-23:48 UT) and flaring (1985 September 7 21:00-22:12 and 23:47-00:37) intervals (see Fig. 2). In order to determine which of the spectral components is responsible for the flaring behavior, the two spectra were simultaneously fit with the same model and the model parameters were constrained to have the same values for both fits. If significant spectral variability is present, this procedure will give a poor fit because the parameter values will converge to their mean values. The model used was the Mitsuda et al. (1984) multicolor blackbody disk model with an additional power-law component. Unsurprisingly, the model is unable to simultaneously fit both the flaring and non-flaring spectra and a minimum χ^2/dof of 1023/245 is obtained. To determine which of the spectral components is responsible for this poor fit, each parameter was allowed to vary independently, one at a time. If either of the parameters associated with the multicolor blackbody disk model or N_H is allowed to vary in this way, acceptable fits are still not obtained with e.g. a χ^2/dof of 960/244 when T_{in} is allowed to vary independently. In contrast, if either the power-law index or normalization is allowed to vary separately, acceptable fits are obtained with χ^2/dof of 219/244 and 312/244 for the independent power-law index and normalization fits, respectively. This indicates that variations in the power-law component are responsible for the intensity variability. This is in agreement with the *hardness* and *softness* ratio analysis presented in section 2.2 which indicates that the source was more variable at higher energies during the 1985 September 7 observation. The slightly better fit obtained when the power-law index rather than the normalization is allowed to vary separately, suggests that variations in power-law slope are more likely responsible for the variability than power-law intensity variations. We caution however, against over interpreting these results since they are dependent on the assumed spectral model.

2.5. Distance and luminosity

Assuming the flux observed during the first observation corresponds to a source luminosity of 10^{38} ergs s^{-1} and that the observed absorption is interstellar, we estimate the distance of

EXO 1846-031 to be 7 kpc. This assumed luminosity value is comparable to the maxima observed from a number of *ultra-soft* transients (e.g. Tanaka 1992). Since we probably did not observe the system at its peak intensity, this distance estimate is only approximate and we await an optical identification in order to better constrain the distance. It is interesting to note that Ginga discovered four X-ray pulsars and three hard X-ray sources within a few degrees of the position of EXO 1846-031 (Koyama et al. 1990). These sources have values of N_H of $10^{22}-5\times10^{23}$ atoms cm^{-2} and Koyama et al. suggest that they are associated with the 5 kpc galactic arm that is located at a distance of 10 kpc. The distance, position and N_H derived above for EXO 1846-031 are also consistent with such a location.

3. Discussion

There are now about a dozen X-ray binaries that are suspected to be black holes (see Tanaka 1992 for a review). The best candidates are the low-mass systems for which the mass functions have been determined to be $\gtrsim 3M_\odot$ from optical measurements and the well studied massive binaries Cyg X-1, LMC X-1 and LMC X-3. In the case of EXO 1846-031, the *ultra-soft* spectral shape combined with a power-law at higher energies, the irregular variability observed from the power-law component, the time scale of the outburst decay and the lack of a bright optical counterpart are all properties shared with the well established candidate black hole systems such as A 0620-00, GS 1124-68 and GS 2000+25. Based on the similarity in these properties, we propose that EXO 1846-031 should also be considered a candidate black hole system.

Short ($\lesssim$ 100 s) timescale intensity variability has been detected from a number of *ultra-soft* transients. In most cases this variability seems to be associated with the hard component. The transients GS 2000+25 and GS 1124-68 are good examples of this, both exhibiting comparable amounts of variability to EXO 1846-031 and having a similar dependence of the amount of variability on energy (Ebisawa 1991; Ogawa 1992). The association of this variability with the hard component is perhaps unsuprising given that a number of black hole candidates such as Cyg X-1 and GX 339-4 exhibit rapid intensity flickering in their low-states, where only the hard power-law component is detected (e.g. Miyamoto 1992). In contrast, the *ultra-soft* transients 4U 1630-47 shows the opposite energy dependence, and the soft component is a factor $\sim$ 2 more variable than the hard component (Parmar et al. 1986). A common feature of the short term variability of these systems is the large variations in its intensity. In the case of EXO 1846-031 this is at least a factor 6. During an outburst from GS 2000+25 even more extreme behavior was observed, with the amount of variability varying by at least a factor 15 (Ebisawa 1991). The reason for these changes is unknown.

We obtain equally good fits to the soft component using cutoff power-law and multicolor blackbody disk models and cannot therefore distinguish between them. The multicolor blackbody disk model has been successfully fit to the spectra of a number of black hole candidates and neutron stars systems (see e.g. Tanaka 1992). For the black hole systems the values of $R_{in}(\cos\theta)^{0.5}$ are systematically a factor three or four higher than the neutron star systems with typical values of $\sim$ 30 km. This is comparable to the mean value derived here emphasizing the similarity between the systems that are considered to be firm black hole candidates and EXO 1846-031. Perhaps more importantly, fits of the same model to the spectra of the transient systems GS 2000+25 (Tanaka 1992) and GS 1124-68 (Kitamoto et al. 1992) reveal that the values of $R_{in}(\cos\theta)^{0.5}$ remain unchanged while the flux decreased by more than an order of magnitude. This invariance of $R_{in}(\cos\theta)^{0.5}$ is also found from LMC X-3, but for a smaller range of luminosity (Ebisawa et al. 1991). The results presented here for EXO 1846-031, while derived from only three observations that span a factor of $\sim$ 7 in luminosity, strengthens the view that the constancy of $R_{in}(\cos\theta)^{0.5}$ may be universal in *ultra-soft* transients. However, fits to the physically more realistic gas pressure dominated accretion disk model also show the same effect (although the fits are of poorer quality) implying that at least one other accretion disk model has the same property. It is important that other accretion disk spectral models are fit to the high-quality Ginga spectra obtained from a number of *ultra-soft* transients in order to better understand the applicability of the various models.

4. Conclusions

We have monitored the evolution in properties of a previously uncatalogued *ultra-soft* X-ray transient EXO 1846-031 during part of an outburst in 1985 April-September when the intensity decreased by a factor $\sim$ 7. The principle results are:

1. The X-ray spectrum of EXO 1846-031 can be fit with a combination of an *ultra-soft* component and a power-law high energy tail that extends to at least 25 keV. The *ultra-soft* component can be successfully modeled by a cutoff power-law or by a multicolor blackbody disk spectrum.
2. The results of fits to the multicolor blackbody model indicate that during the outburst T_{in} decreases from 0.96 to 0.69 keV, while $R_{in}(\cos\theta)^{0.5}$ remains at $\sim$ 22 km for a distance of 7 kpc. At least one other accretion disk spectral model is able to account for these changes by the variation in a single parameter.
3. During one of three EXOSAT observations, EXO 1846-031 showed significant excess variability with a characteristic time scale in the 1–10 keV band of 50 s. This variability is probably associated with the high-energy power-law spectral component.
4. The similarity in properties between EXO 1846-031 and the black hole systems suggests that EXO 1846-031 should also be considered a member of this class.

Acknowledgements. We thank the EXOSAT Observatory team for help with these observations. Andy Pollock is thanked for assistance in interpreting the EXOSAT ME slew data.

References

Bahcall J.N., 1978, ARA&A 16, 241
Callanan P.J., Charles P.A., 1991, MNRAS 249, 573
Casares J., Charles P.A., Naylor T., 1992, Nat 355, 614
de Korte P.A.J., Bleeker J.A.M., den Boggende A.J.F., et al., 1981, Space Sci. Rev. 30, 495
Cominsky L., Jones C., Forman W., Tannanbaum H., 1978, ApJ 224, 46
Ebisawa K., 1991. PhD thesis. University of Tokyo
Ebisawa K., Mitsuda K., Hanawa T., 1991, ApJ 367, 213
Gottwald M., Haberl F., Parmar A.N., White N.E., 1986, ApJ 308, 213
Gottwald M., Steinle H., Graser U., Pietsch W., 1991, A&AS 89, 369
Kitamoto S., Tsunemi H., Miyamoto S., Hayashida K., 1992, ApJ 394, 609
Koyama K., Kawada M., Kunieda H., et al., 1990, Nat 343, 148
Landolt A.U., 1992, AJ 104, 320
Maraschi L., Huckle H., Ives J., Sanford P.W., 1976, Nat 263, 34
McClintock J.E., Remillard R.A., 1986, ApJ 308, 110
Mitsuda K., Inoue H., Koyama K., et al., PASJ 36, 741
Miyamoto S., Kimura K., Kitamoto S., Dotani T., Ebisawa K., 1991, ApJ 383, 784
Miyamoto S., Kitamoto S., Iga S., Terada K., 1992, ApJ 391, L21
Morisson D., McCammon D., 1983, ApJ 270, 119
Ogawa M., 1992, PhD Thesis. Rikkyo University
Nagase F., 1989, PASJ 41, 1
Parmar A.N., Stella L. White N.E., 1986, ApJ 304, 664
Parmar A.N., White N.E., 1985, IAU Circ. 4051
Parmar A.N., White N.E., Stella L., 1989a, ApJ 338, 359
Parmar A.N., White N.E., Stella L., Izzo C., Ferri P., 1989b, ApJ 338, 373
Peacock A., Andresen R.D., Manzo G.T., et al., 1981, Space Sci. Rev. 30, 525
Remillard R.A., McClintock J.E., Bailyn C., 1991, ApJ 399, L145
Shakura N.I., Sunyaev R.A., 1973, A&A 24, 337
Stella L., Rosner R., 1984, ApJ 277, 312
Sutherland P.G., Weisskopf M. C., Kahn S.M., 1978, ApJ 219, 1029
Sunyaev R., Titarchuk L.G., 1980, A&A 86, 121
Sunyaev R., Churazov E., Gilfanov M., et al., 1992, ApJ 389, L75
Tanaka Y., 1992, Black Hole Binaries. In: Makino F. Nagase F. (eds.) Proc. of the Ginga Memorial Symposium. ISAS, Tokyo, p. 19
Turner M.J.L., Smith A., Zimmermann H.U., 1981, Space Sci. Rev. 30, 513
Warwick R.S., Marshall N., Fraser G.W., et al., 1981, MNRAS 197, 865
White N.E., Kaluzienski J.J., Swank J.H., 1984, The Spectra of X-ray Transients. In: Woosley S. (ed.) High Energy Transients in Astrophysics. AIP, 31
White N.E., Peacock A., 1985, The EXOSAT Observatory. In: Pallavicini R. White N.E. (eds.) X-ray Astronomy with EXOSAT. Italian Astronomical Society, Firenze, p. 1
White N.E., Stella L., Parmar A.N., 1988, ApJ 324, 363
Wilson C.K., Rothschild R.E., 1983, ApJ 274, 717
Wood K.S., Meekins J.F., Yentis D.J., et al., 1984, ApJS 56, 507

This article was processed by the author using Springer-Verlag LaTeX A&A style file version 3.